

# RSUD20K: A DATASET FOR ROAD SCENE UNDERSTANDING IN AUTONOMOUS DRIVING

*Hasib Zunair, Shakib Khan, and A. Ben Hamza*

Concordia University, Montreal, QC, Canada

## ABSTRACT

Road scene understanding is crucial in autonomous driving, enabling machines to perceive the visual environment. However, recent object detectors tailored for learning on datasets collected from certain geographical locations struggle to generalize across different locations. In this paper, we present RSUD20K, a new dataset for road scene understanding, comprised of over 20K high-resolution images from the driving perspective on Bangladesh roads, and includes 130K bounding box annotations for 13 objects. This challenging dataset encompasses diverse road scenes, narrow streets and highways, featuring objects from different viewpoints and scenes from crowded environments with densely cluttered objects and various weather conditions. Our work significantly improves upon previous efforts, providing detailed annotations and increased object complexity. We thoroughly examine the dataset, benchmarking various state-of-the-art object detectors and exploring large vision models as image annotators.

**Index Terms**— Object detection; road scene understanding; large vision models; autonomous driving

## 1. INTRODUCTION

Effectively understanding road scenes involves overcoming challenges related to illumination, viewpoint differences, and background clutter, which significantly impact object detection performance, especially in cases of occluded and small objects. Addressing these issues is crucial for deploying robust perception systems, ensuring safe driving of autonomous vehicles, and averting accidents in real-world scenarios. Recent approaches to road scene understanding are data-driven learning-based methods like YOLO [1], Faster R-CNN [2] and DETR [3], and have become prevalent in modern autonomous driving systems. Publicly available datasets such as CityScapes [4], Mapillary Vistas [5], KITTI Vision Benchmark Suite [6], BDD100K [7], and Waymo Open Dataset [8] have paved the path toward autonomous driving. However, learning-based methods trained on these datasets may not generalize well to new geographic locations such as Bangladesh or India. Since data labeling is both time consuming and costly, a workaround to this problem is to leverage the zero-shot capabilities of recent vision foundation models such as Grounding DINO [9], OWL-ViT [10], DETIC [11] and SAM [12] to quickly annotate new data using

prompt engineering. While automatic data labeling could potentially save time and reduce cost, it is still questionable as to how good supervised models would perform when trained on data generated using foundation models.

To address the aforementioned issues and establish a platform to enable autonomous driving progress across various geographical locations, we propose a **Road Scene Understanding Dataset (RSUD20K)** comprised of over 20K high-resolution images paired with 130K bounding box annotations of 13 objects captured from the perspective of a driving vehicle on Bangladesh roads. As shown in Fig. 1, images consist of real-world scenarios like diverse roads, narrow streets, highways and objects from different viewpoints. Further, scenes include crowded environments and various weather conditions. The main contributions of this work can be summarized as follows: **(1)** We introduce RSUD20K, a novel dataset for road scene understanding, providing detailed annotations; **(2)** we benchmark state-of-the-art object detectors on RSUD20K, demonstrating the challenges in the task; and **(3)** we adopt a data-centric approach and assess the performance of large vision models as image annotators in zero-shot scenarios.

## 2. RELATED WORK

**Bangladesh Street View Datasets.** DhakaAI [13] presents a dataset with 3953 images and 24368 bounding box annotations across 21 classes. However, issues such as mislabeling and inconsistent image quality have been identified [14]. Poribohon-BD [15] consists of 9058 images and bounding box labels for 15 vehicle classes. However, some objects such as boats are unrelated to autonomous driving and the dataset’s multi-class vehicle category has limited samples. MVINet [16] introduce a dataset for multi-class classification with 10 vehicle types and 100 images per class. This dataset is, however, not publicly available. Table 1 provides a detailed comparison between RSUD20K and these datasets.

**Object Detectors.** Most existing object detection methods can be categorized into one- and two-stage detectors. One-stage detectors, such as YOLO [1], single shot detector (SSD)[17], RetinaNet[18], CenterNet [19], and DETR [3], directly generate candidate bounding boxes and predictions in a single processing step, making them suitable for real-time detection in autonomous driving. However, their performance notably degrades when detecting dense and small objects. On



**Fig. 1: RSUD20K for road scene understanding.** The dataset consists of a total of **20334** images with **130K** bounding box annotations of **13** different objects. Images are captured from the driving perspective of diverse road scenes, objects from different viewpoints, occlusions, as well as under various weather conditions.

**Table 1: Comparison of RSUD20K with existing Bangladesh road scene understanding datasets.** While the other datasets are mainly for traffic detection and recognition of vehicles, RSUD20K is built for the application of autonomous driving.

Specifications	Dhaka-AI [13]	Poribohon-BD [15]	MVINet [16]	RSUD20K (Ours)
Image Resolution	1920 × 1080	1920 × 1080	128 × 128	1920 × 1080
Number of Images	3953	9058	17000	20000
Number of Classes	21	15	17	13
Target Task	Object Detection	Classification	Multi-class Classification	Object Detection
Annotation Type	2D bounding boxes	2D bounding boxes	2D bounding boxes	2D bounding boxes
Public	✓	✓	✗	✓
Application	Traffic Detection	Vehicle Classification	Vehicle Classification	Autonomous Driving

the other hand, two-stage detectors like R-CNN [20], Fast R-CNN [21], Faster R-CNN [2], and Mask R-CNN [22] employ object regions using deep features before classifying the objects, resulting in higher detection accuracy.

**Large Vision Models (LVMs).** The open-set capabilities of LVMs enable interpretation of objects unseen during training (i.e., zero-shot). Grounding DINO [9] is an open-set object detector based on the Transformer detector DINO, featuring grounded pre-training to detect arbitrary objects from category names or referring expressions. OWL-ViT transfers image-level contrastive pre-training to open-set object detection. DETIC [11] extends open-set detection to over 20K classes by training classifiers on image-level data. SAM [12] introduces a task and promptable model for image segmentation, trained on a dataset of 1B masks and 11M images. LVMs can be used for automatic data annotation (pseudo-labeling), potentially saving time and reducing cost. However, the performance of supervised models trained on datasets created using LVMs remains unclear.

### 3. ROAD SCENE UNDERSTANDING DATASET

We start with the problem formulation, and then delve into the data engine and analysis of our RSUD20K dataset. The key steps of our data engine are presented in Fig. 2.

**Problem Statement.** Let  $\mathcal{D} = \{(\mathbf{I}_i, \mathbf{B}_i)\}_{i=1}^N$  be a training set of  $N$  labeled images  $\mathbf{I}_i \in \mathcal{X}$  and their ground-truth bounding box annotations  $\mathbf{B}_i$ . Each bounding box represents the coordinates of the top-left and bottom-right corners of the bounding box in the image, denoted as  $(x_i^{\min}, y_i^{\min}, x_i^{\max}, y_i^{\max})$ . The task of object detection is to learn a model  $f_{\theta} : \mathcal{X} \rightarrow \mathcal{Y}$ , where  $\theta$  is a set of learnable parameters. In this context,  $\mathcal{Y}$  represents the set of bounding box annotations for the detected objects. Given a test image  $\mathbf{I}$ , the trained model predicts a set of bounding boxes  $\mathbf{B}_p$ , where each predicted bounding box is denoted as  $(x_p^{\min}, y_p^{\min}, x_p^{\max}, y_p^{\max})$ .

#### 3.1. Data Engine

**Image Collection.** We created our RSUD20K dataset by collecting a diverse set of over 80 video sequences with a resolution of 1920 × 1080 featuring street scenes, recorded using an in-car dashboard-mounted camera. To ensure data integrity and avoid leakage, we manually grouped the video sequences into training, validation and test sets, balancing scenes from different environments such as outskirts and cities, along with varying weather conditions like nighttime or rainy scenes. Each video sequence, lasting 2-5 minutes, showcases different roads, streets, and highways in the same area. The group partitioning resulted in 54 training, 19 validation, and 11 test video sequences. From these sequences, we sampled images

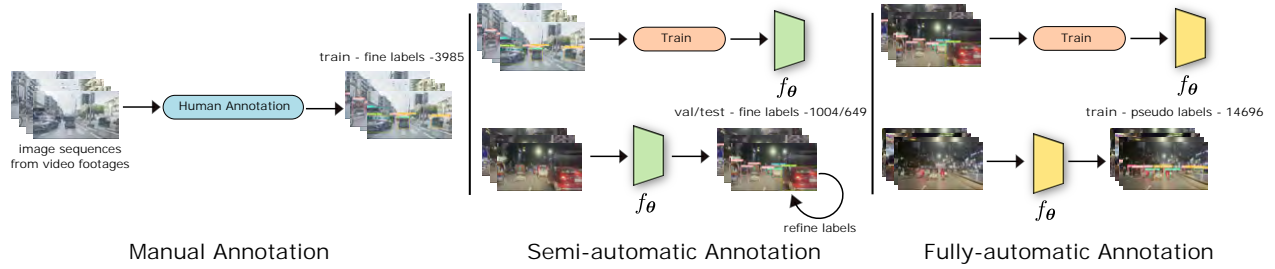


**Fig. 2: Overview of our data engine used to create RSUD20K.** We use a three-stage approach, where  $f_\theta$  is YOLOv6-M6 detector trained to predict bounding boxes and class labels of objects.

for training, validation, and test sets, with 400, 60, and 60 frames respectively per video. This sampling strategy yielded a total of 23,246 images, with 18,762 training images, 1,008 validation images and 656 test images.

**Manual Annotation.** In this stage, we follow a process similar to traditional multi-class object detection. A team of professionals manually annotates 4,000 randomly sampled images from the training set by delineating bounding box regions around objects of interest and assigning class names using the open-source Label Studio annotation tool<sup>1</sup>. The focus is on creating a dataset for autonomous driving, specifically for understanding driving scenarios. We identify 13 classes of interest: *person, rickshaw, rickshaw van, auto rickshaw, truck, pickup truck, private car, motorcycle, bicycle, bus, micro bus, covered van, and human hauler*. Annotators are instructed to draw bounding boxes tightly around these objects, ensuring at least one bounding box with a class label per image. Images without objects from the specified 13 classes are discarded. If an object is occluded by more than roughly 50%, it is also omitted from annotation. In cases where the object is visible, but still partially occluded, a box is drawn around the visible portion. The constraint to draw tight boxes is relaxed in dense and cluttered scenes to capture real-world characteristics. On average, the annotation time per image with multiple bounding boxes is 48 seconds. This stage yields 3,985 images with corresponding bounding box labels for a total of 13 different classes.

**Semi-Automatic Annotation.** In this stage, we aim to label the validation and test set image collections, consisting of 1,008 and 656 images, respectively. Initially, we train YOLOv6-M6 using the labeled data from manual annotation. Through inference, we generate bounding box predictions for the 13 classes within the validation and test sets in a pseudo-labeling fashion. Images with null predictions are excluded. Subsequently, we present the pseudo-labeled images to annotators for label refinement, which involves adjusting bounding boxes tightly around objects and correcting any inaccurate labels predicted by the model. This stage serves two main purposes: (i) to establish gold standard labels for the validation

and test sets for model evaluation, and (ii) to expedite the labeling process by leveraging model predictions. The average annotation time per image is significantly reduced from 48 seconds to 8 seconds, representing a six-fold increase in efficiency compared to manual human annotation. This approach is accurate, efficient, cost-effective, and scalable, playing a crucial role in building high-quality datasets. Finally, we generate refined validation and test sets comprising 1,004 and 649 images, respectively, each with corresponding bounding box labels for the 13 classes. These sets, combined with the training set, form the RSUD5K dataset.

**Fully Automatic Annotation.** In this final stage of our annotation process, automation takes center stage, leveraging a semi-supervised approach [23]. We employ YOLOv6-M6, previously trained on images with bounding box labels in RSUD5K to pseudo-label unlabeled images. The model’s predictions for bounding boxes across the 13 classes are generated for the remaining 14,762 images. After filtering out images with null predictions, we obtain 14,696 pseudo-labeled images. These are seamlessly integrated into the RSUD5K training set, resulting in the expanded RSUD20K dataset, which now comprises a total of 20,334 images.

### 3.2. Data Analysis

**Overview of Images and Bounding Boxes.** Each image in our RSUD20K dataset is annotated with bounding boxes and their class labels, featuring annotations with multiple instances at various levels of granularity. RSUD20K encapsulates diverse driving scenes captured from the perspective of a driving vehicle, encompassing objects in different viewpoints and densely cluttered areas leading to significant occlusions. Notably, the dataset includes driving scenes at night and in rainy conditions, distinguishing it from existing autonomous driving datasets.

**Annotation Statistics.** We aim to answer two questions regarding class distribution: “How many images in each dataset split belong to a particular class?” and “How many bounding box instances exist for each class?”. Fig. 3 presents these statistics at both the image and instance levels. In Fig. 3 (top), we depict the distribution of images containing differ-

<sup>1</sup><https://labelstud.io>

ent classes in all data splits. Notice the data imbalance, with over-represented classes like *person*, *rickshaw*, *private car*, and under-represented classes such as *pickup truck*, *covered van*, *human hauler*. Fig. 3 (bottom) illustrates the distribution of bounding box instances for each class. The training set exhibits the highest number of instances for *person* (over 30K boxes) and the lowest for *human hauler* (455 instances), indicating significant imbalance. In summary, RSUD20K comprises 130K bounding box instances across 13 classes, distributed as 118,810, 7,385, and 3,805 instances in the training, validation, and test sets, respectively.

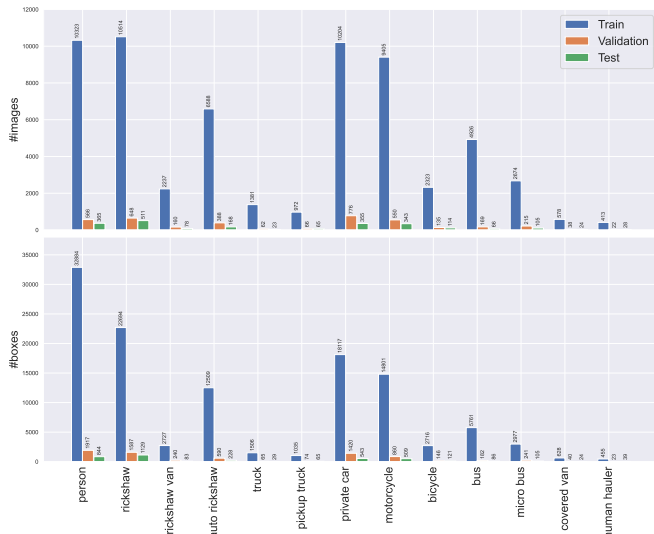


**Fig. 3: Dataset statistics of RSUD20K.** Image level annotations statistics (top) and bounding box instances (bottom).

**Object Coverage.** Understanding objects encountered on the streets accurately is crucial for road scene comprehension and marks the initial step toward autonomous driving. Annotations include various object viewpoints (e.g., front, back, side), addressing the challenge posed by narrow, lane-less roads, where recognizing objects from different perspectives is vital. This distinguishes our dataset from existing ones. We also focused on establishing entry-level categories in lieu of fine-grained recognition, which involves distinguishing subordinate categories. For instance, our dataset includes fine-grained classes such as *rickshaw* and *rickshaw van*.

**Scene Coverage.** We collected diverse video sequences capturing various road/driving scenes, encompassing daylight, nighttime and rainy weather, marking distinctive features compared to existing datasets. Our dataset also includes scenes from heavily crowded areas and outskirts of cities, and accounts for varying weather conditions (e.g., extreme sunny days causing glare), resulting in illumination challenges.

**Density of Bounding Boxes.** In Fig. 4, we examine the distribution of bounding boxes in RSUD20K. On average, most images in the dataset contain around 4-9 objects. Over 3.5K

images exhibit over 10 densely cluttered objects. The most frequent number of bounding boxes per image is 6, observed in 2765 images, followed by 2618 images with 5 bounding boxes and 2352 images with 7 bounding boxes. There are also 988 images with 10 bounding boxes and 628 images with 8 bounding boxes, and one image with 23 bounding boxes. This analysis provides valuable insights into the diversity and distribution of bounding box annotations in RSUD20K.

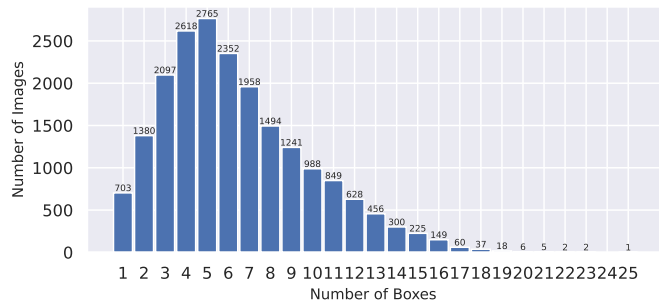


**Fig. 4: Distribution of box instances in RSUD20K.** Most images have a total of roughly 5 to 8 bounding boxes, demonstrating that there are many objects in the driving scenes.

**Challenges.** RSUD20K presents several challenges: (i) It features scenes with no typical lane markings and narrow streets, which are uncommon in existing datasets; and (ii) certain vehicles like *rickshaw* and *rickshaw van* are human-powered, posing recognition difficulties as models may easily misclassify them as persons. Also, most images depict crowded street scenes with densely cluttered objects, leading to heavy occlusions. Certain scenes were captured both in daylight and nighttime, including rainy conditions, thereby introducing challenges related to varying illumination.

## 4. EXPERIMENTS

### 4.1. Experimental Setup

**Baselines.** We benchmark recent state-of-the-art object detectors on RSUD20K, including YOLOv6 and YOLOv8 [1], Transformer-based detectors DETR [3] and RTMDET [24]. We also compare the performance of supervised models when trained with labels generated by LVMs, including Grounding DINO [9], OWL-ViT [10], SAM [12], and DETIC [11].

**Evaluation Metrics.** We employ mean average precision (mAP), a standard metric in object detection, as our primary evaluation measure. Given the imbalanced nature of our dataset, we also report per-class mAP results.

### 4.2. Benchmarking Results

We report the detection performance of various object detectors on RSUD20K, and explore the zero-shot capabilities of LVMs as image annotators to train supervised models. Dataset, code and pre-trained models will be made public.

**Object Detection Results.** We compare the performance of various state-of-the-art object detection methods, and the results are reported in Table 2. We find that the best performing models are YOLOv6 and YOLOv8. Transformer-based methods like DETR yield lower detection performance, with 49.9 mAP compared to the best performing model YOLOv6-L achieving 73.7 mAP. Notably, objects operated by a person, such as rickshaws, rickshaw vans, and bicycles, showcase relatively efficient detection. However, certain classes like rickshaw van, truck, and pickup truck demonstrate lower mAPs (54.0, 50.7, and 67.9, respectively). This is because these object classes have sub-ordinate categories, resulting in size and shape variations, thus requiring fine-grained recognition. We also present qualitative examples in Fig. 5.

**LVMs as Image Annotators.** We explore the use of LVMs for automatic image annotation to train supervised models, comparing their efficacy against human labels. Our data-centric approach keeps the algorithm fixed while altering the dataset, specifically the bounding box labels. We evaluate LVMs for data generation, aiming to determine if they can efficiently annotate data without compromising the detection performance. To automatically generate labels using LVMs, we first create a dictionary of class labels and descriptions by prompting a large language model to describe each class. Then, we input this dictionary and images from the training set of RSUD5K into various LVMs, including Grounding DINO, OWL-ViT, SAM and DETIC, which produce bounding box labels in a few hours. Finally, we train different object detection models on these LVM-generated datasets and compare their results on the test set (see Table 3). Our findings reveal that while LVMs efficiently annotate images for specialized tasks, the performance significantly drops across all object detection models compared to ground-truth labels. This is attributed to the distinctive nature of our dataset, featuring objects that are not commonly seen in other geographical locations (e.g., North America or Europe). Even DETIC, an object detector trained to detect 20K classes, exhibits suboptimal results in this specific context.

### 4.3. Ablation Study

We analyze how pseudo-labeled data affects model performance, and quantify the impact of increasing model capacity.

**Data Scaling.** Fig. 6 shows the benefit of using pseudo-labeled data we created in the fully-automatic stage, resulting in consistently improved detection performance across various object detectors in both validation and test sets.

**Model Scaling.** We conduct experiments to investigate the impact of increasing model capacity on RSUD20K. As shown in Table 4, the detection performance increases as the model is scaled up, in both validation and test sets.

## 5. CONCLUSION

We introduced RSUD20K, a novel dataset for road scene understanding, featuring 20K high-resolution images and 130K bounding box annotations across 13 object classes. These images capture diverse viewpoints, crowded environments, and under various weather conditions, presenting real-world scenarios. The significance of RSUD20K is underscored by its challenging nature, which remains unresolved even with state-of-the-art object detectors. The dataset not only serves as a benchmark for addressing existing vision challenges, but also provides a platform for developing road scene understanding algorithms tailored for autonomous driving.

## 6. REFERENCES

- [1] Juan Terven and Diana Cordova-Esparza, “A comprehensive review of YOLO: From YOLOv1 to YOLOv8 and beyond,” *arXiv preprint arXiv:2304.00501*, 2023.
- [2] Shaoqing Ren, Kaiming He, Ross Girshick, and Jian Sun, “Faster R-CNN: Towards real-time object detection with region proposal networks,” in *Advances in Neural Information Processing Systems*, 2015, vol. 28.
- [3] Nicolas Carion, Francisco Massa, Gabriel Synnaeve, Nicolas Usunier, Alexander Kirillov, and Sergey Zagoruyko, “End-to-end object detection with transformers,” in *Proc. European Conference on Computer Vision*, 2020, pp. 213–229.
- [4] Marius Cordts, Mohamed Omran, Sebastian Ramos, Timo Rehfeld, Markus Enzweiler, Rodrigo Benenson, Uwe Franke, Stefan Roth, and Bernt Schiele, “The cityscapes dataset for semantic urban scene understanding,” in *Proc. IEEE Conference on Computer Vision and Pattern Recognition*, 2016.
- [5] Gerhard Neuhold, Tobias Ollmann, Samuel Rota Buló, and Peter Kotschieder, “The mapillary vistas dataset for semantic understanding of street scenes,” in *Proc. IEEE International Conference on Computer Vision*, 2017, pp. 4990–4999.
- [6] Andreas Geiger, Philip Lenz, and Raquel Urtasun, “Are we ready for autonomous driving? the KITTI vision benchmark suite,” in *Proc. IEEE Conference on Computer Vision and Pattern Recognition*, 2012.
- [7] Fisher Yu, Haofeng Chen, Xin Wang, Wenqi Xian, Yingying Chen, Fangchen Liu, Vashisht Madhavan, and Trevor Darrell, “BDD100K: A diverse driving dataset for heterogeneous multitask learning,” in *Proc. IEEE Conference on Computer Vision and Pattern Recognition*, 2020, pp. 2636–2645.
- [8] Pei Sun, Henrik Kretzschmar, Xerxes Dotiwalla, Aurelien Chouard, Vijaysai Patnaik, Paul Tsui, James Guo,

**Table 2: Performance comparison of state-of-the-art object detectors on RSUD20K in terms of mean and per-class mean average precision (mAP).** The best results are in bold, and the second best are underlined.

Method	YOLOv8-L	YOLOv8-M	YOLOv8-S	RTMDet	DETR	YOLOv6-S	YOLOv6-M	YOLOv6-L
Input Size	640 × 640	640 × 640	640 × 640	640 × 640	640 × 640	640 × 640	640 × 640	640 × 640
Params (M)	43.7	25.9	11.2	4.8	41.3	18.5	34.9	59.6
person	<b>73.6</b>	71.7	70.2	63.5	59.2	69.7	<u>72.8</u>	72.5
rickshaw	<b>88.3</b>	<u>87.3</u>	86.0	81.4	78.4	85.2	86.6	86.6
rickshaw van	47.4	<u>53.8</u>	52.8	49.8	33.4	45.9	51.5	<b>54.0</b>
auto rickshaw	<b>88.5</b>	88.3	87.2	83.2	80.2	85.9	88.7	<u>88.4</u>
truck	34.8	40.7	<u>50.0</u>	36.5	17.7	57.1	42.3	<b>50.7</b>
pickup truck	<b>67.9</b>	<u>63.1</u>	59.4	56.7	13.6	62.6	62.7	62.3
private car	<b>87.9</b>	87.6	86.5	81.1	77.8	85.9	87.2	<u>87.7</u>
motorcycle	77.1	76.9	75.1	68.9	67.1	75.2	<u>77.5</u>	<b>77.8</b>
bicycle	73.1	71.0	69.4	64.5	56.1	69.9	<u>73.9</u>	<b>74.5</b>
bus	64.1	60.6	65.1	60.8	41.5	70	<u>73.8</u>	<b>75.3</b>
micro bus	86.7	<u>87.1</u>	76.8	81.0	48.8	86.0	<b>88.1</b>	85.9
covered van	53.5	<u>69.6</u>	53.5	62.0	21.9	71.5	<u>71.6</u>	<b>78</b>
human hauler	67.1	75.3	70.7	60.8	57.0	71.4	<u>78.9</u>	<b>79.0</b>
Mean	70.4	71.8	69.4	65.4	49.9	72.0	<u>73.5</u>	<b>73.7</b>



**Fig. 5: Visualization comparison of predictions by state-of-the-art object detectors on RSUD20K.** First two rows show occlusions and viewpoint differences. Second two rows show cases of various weather conditions. Zoom-in for better details.

**Table 3: Performance comparison of large vision models trained on RSUD5K in terms of %mAP.**

Method	YOLOv6-S	YOLOv6-M	YOLOv6-L
Grounding DINO [9]	9.0	8.8	9.3
OWL-ViT [10]	10.1	9.9	10.7
SAM [12]	12.3	11.8	13.2
DETIc [11]	<u>14.8</u>	<u>14.4</u>	<u>15.8</u>
Supervised	<b>66.3</b>	<b>65.7</b>	<b>67.2</b>

**Table 4: Model scaling performance on RSUD20K.** Increasing model capacity yields higher detection performance.

Method	Params (M)	FLOPs (G)	Validation (%mAP)	Test (%mAP)
YOLOv6-S	18.5	45.3	65.4	72.0
YOLOv6-M	34.9	85.8	68.6	73.5
YOLOv6-L	59.6	150.7	67.3	73.7
YOLOv6-M6	79.6	379.5	<b>70.3</b>	<b>77.9</b>



(a) mAP on RSUD20K val set. (b) mAP on RSUD20K test set.  
**Fig. 6: Performance comparison of models trained using pseudo labeled data on RSUD20K validation and test sets.** Pseudo-labels consistently improve detection performance different object detection models.

Yin Zhou, Yuning Chai, Benjamin Caine, et al., “Scalability in perception for autonomous driving: Waymo open dataset,” in *Proc. IEEE Conference on Computer Vision and Pattern Recognition*, 2020, pp. 2446–2454.

- Zhang, Jie Yang, Chunyuan Li, Jianwei Yang, Hang Su, Jun Zhu, et al., “Grounding DINO: Marrying DINO with grounded pre-training for open-set object detection,” *arXiv preprint arXiv:2303.05499*, 2023.
- [10] M Minderer, A Gritsenko, A Stone, M Neumann, D Weissenborn, A Dosovitskiy, A Mahendran, A Arnab, M Deghani, Z Shen, et al., “Simple open-vocabulary object detection with vision Transformers,” in *Proc. European Conference on Computer Vision*, 2022.
- [11] Xingyi Zhou, Rohit Girdhar, Armand Joulin, Philipp Krähenbühl, and Ishan Misra, “Detecting twenty-thousand classes using image-level supervision,” in *Proc. European Conference on Computer Vision*, 2022, pp. 350–368.
- [12] Alexander Kirillov, Eric Mintun, Nikhila Ravi, Hanzi Mao, Chloe Rolland, Laura Gustafson, Tete Xiao, Spencer Whitehead, Alexander C Berg, Wan-Yen Lo, et al., “Segment anything,” *arXiv preprint arXiv:2304.02643*, 2023.
- [13] ASM Shihavuddin and Mohammad Rifat Ahmmad Rashid, “DhakaAI,” in *Harvard Dataverse*, 2020.
- [14] Raian Rahman, Zadid Bin Azad, and Bakhtiar Hasan, “Densely-populated traffic detection using YOLOv5 and non-maximum suppression ensembling,” in *Proc. International Conference on Big Data, IoT, and Machine Learning*, 2022, pp. 567–578.
- [15] Shaira Tabassum, Sabbir Ullah, Nakib Hossain Al-Nur, and Swakkhar Shatabda, “Poribohon-BD: Bangladeshi local vehicle image dataset with annotation for classification,” *Data in Brief*, vol. 33, 2020.
- [16] Tanvir Ahmed, Farzana Sharmin Mou, and Abu Anas Ibn Samad, “A deep learning based Bangladeshi vehicle classification using fine-tuned multi-class vehicle image network (MVINet) model,” in *Proc. International Conference on Next-Generation Computing, IoT and Machine Learning*, 2023, pp. 1–6.
- [17] Wei Liu, Dragomir Anguelov, Dumitru Erhan, Christian Szegedy, Scott Reed, Cheng-Yang Fu, and Alexander C Berg, “SSD: Single shot multibox detector,” in *Proc. European Conference on Computer Vision*, 2016, pp. 21–37.
- [18] Tsung-Yi Lin, Priya Goyal, Ross Girshick, Kaiming He, and Piotr Dollár, “Focal loss for dense object detection,” in *Proc. IEEE International Conference on Computer Vision*, 2017, pp. 2980–2988.
- [19] Kaiwen Duan, Song Bai, Lingxi Xie, Honggang Qi, Qingming Huang, and Qi Tian, “CenterNet: Keypoint triplets for object detection,” in *Proc. IEEE International Conference on Computer Vision*, 2019, pp. 6569–6578.
- [20] Ross Girshick, Jeff Donahue, Trevor Darrell, and Jitendra Malik, “Rich feature hierarchies for accurate object detection and semantic segmentation,” in *Proc. IEEE Conference on Computer Vision and Pattern Recognition*, 2014, pp. 580–587.
- [21] Ross Girshick, “Fast R-CNN,” in *Proc. IEEE International Conference on Computer Vision*, 2015, pp. 1440–1448.
- [22] Kaiming He, Georgia Gkioxari, Piotr Dollár, and Ross Girshick, “Mask R-CNN,” in *Proc. IEEE International Conference on Computer Vision*, 2017, pp. 2961–2969.
- [23] Hasib Zunair, Yan Gobeil, Samuel Mercier, and A. Ben Hamza, “STAR: noisy semi-supervised transfer learning for visual classification,” in *Proc. International Workshop on Multimedia Content Analysis in Sports*, 2021, pp. 25–33.
- [24] Chengqi Lyu, Wenwei Zhang, Haiyan Huang, Yue Zhou, Yudong Wang, Yanyi Liu, Shilong Zhang, and Kai Chen, “RTMDet: An empirical study of designing real-time object detectors,” *arXiv preprint arXiv:2212.07784*, 2022.

## — Supplementary Material —

This supplementary material provides further details on implementation, along with additional experimental results.

### 7. IMPLEMENTATION DETAILS

**Data Processing.** Images are resized to  $640 \times 640$  and standardized to have values between 0 and 1. We only apply basic data augmentation methods such as random flipping and re-sizing crops.

**Model Training.** We used various open-source libraries to train different models. YOLOv6 models are trained using the out-of-the-box open-source library YOLOv6<sup>2</sup>. YOLOv8 models are trained with the Ultralytics<sup>3</sup>. DETR models utilize the MMDetection<sup>4</sup>. For RTMDet, we employ the MMYOLO<sup>5</sup> library from OpenMMLab<sup>6</sup>.

**Model Testing.** After training, the model, when given an image as input, predicts bounding boxes and assigns labels from predefined classes.

**Hardware and Software Details.** We conducted our experiments on a Linux workstation with a processing speed of 4.8Hz and 64GB RAM, featuring a single NVIDIA RTX 3080Ti GPU with 12GB of memory. All algorithms are implemented in PyTorch.

**Labeling Criteria.** The data labeling criteria are as follows:

- *person*: draw boxes on persons only that are walking, not on vehicles.
- *rickshaw*: boxes without person if possible. should be a tight box around the object.
- *rickshaw van*: boxes around any three wheeler vans pulled by humans (e.g. selling vegetables or fruits).
- *auto rickshaw*: any CNG, three wheeler electric vehicles
- *truck*: big or small trucks
- *pickup truck*: blue small vans, other small vans.
- *private car*: any private car (includes jeeps too).
- *motorcycle*: box should not have person if possible.
- *bicycle*: box should not have person if possible.
- *bus*: any bus, small or big.

- *micro bus*: big cars like ambulance or other 7/8 seater cars (also Noah).
- *covered van*: like pickup, but covered.
- *human hauler*: leguna.

In general, we aim for tight boxes around objects. If an object is occluded by more than 50%, we refrain from labeling it. We only draw a tight box if more than 50% of the object is visible. In densely populated scenes, a bit of overlap between boxes is acceptable. Our data labeling process is facilitated using the Label Studio<sup>7</sup> annotation tool.

**Prompt Dictionary.** We use the open-source language model, ChatGPT, to create short descriptions for our 13 objects. These descriptions form a prompt dictionary, guiding how large vision models are instructed. The dictionary includes text captions, serving as descriptions, and the corresponding class names. It specifies the actual labels. ChatGPT is employed to generate these label descriptions using the input prompt: “describe what a class name looks like in 15-20 words.” The generated descriptions are as follows:

- “A person is a living being with a complex physical form, including a head, torso, limbs, and varied appearance based on ethnicity and individual traits.” : “person”
- “A rickshaw is a human-powered or motorized vehicle with a simple frame, seating, and often two or three wheels.” : “rickshaw”
- “A rickshaw van is a motorized three-wheeled vehicle with an enclosed cabin for passengers or goods, and typically a driver upfront.” : “rickshaw van”
- “An auto rickshaw is a compact, three-wheeled motorized vehicle with a cabin for passengers, a driver upfront, and a rear engine.” : “auto rickshaw”
- “A truck is a large, motorized vehicle with a driver’s cabin, cargo area, wheels, and often a distinct front grille.” : “truck”
- “A pickup truck is a smaller motorized vehicle with a driver’s cabin and an open cargo bed in the rear.” : “pickup truck”
- “A private car is a four-wheeled motor vehicle designed for personal transportation, typically with seating for passengers and an enclosed cabin.” : “private car”
- “A motorcycle is a two-wheeled motor vehicle with a seat for a rider and often a pillion seat for a passenger.” : “motorcycle”

---

<sup>2</sup>YOLOv6

<sup>3</sup>ultralytics

<sup>4</sup>MMDetection

<sup>5</sup>MMYOLO

<sup>6</sup>OpenMMLab

---

<sup>7</sup>Label Studio

- “A bicycle is a human-powered vehicle with two wheels, pedals, a frame, handlebars, and a seat for a rider.” : “bicycle”
- “A bus is a large motorized vehicle with a passenger cabin, typically featuring multiple seats, windows, and a distinctive elongated shape.” : “bus”
- “A micro bus is a smaller motorized vehicle, similar to a standard bus but more compact with seating for fewer passengers.” : “micro bus”
- “A covered van is a motorized vehicle with a closed cargo area, often used for transporting goods, and may have a driver’s cabin upfront.” : “covered van”
- “A human hauler is a motorized vehicle designed for transporting passengers, similar to an auto rickshaw or tuk-tuk, with a cabin and driver upfront.” : “human hauler”

These descriptions serve as input prompts for foundation models such as DETIC, Grounding DINO, OWL-ViT, and SAM. Fig. 7 illustrates the image labeling process via prompt engineering, where the pseudo bounding box and class labels are generated using DETIC as an image annotator.

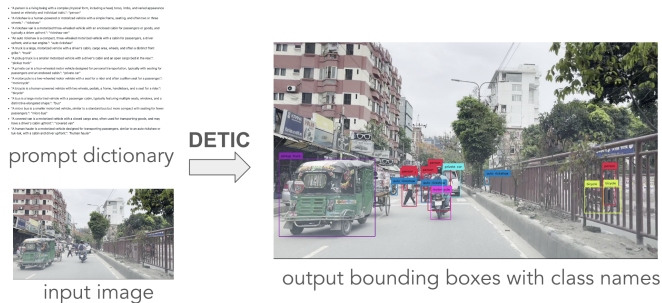


**Fig. 7: Label images via prompt engineering.** Given a prompt dictionary and an input image, a large vision model (i.e., DETIC) generates pseudo bounding box and class labels for our task.

## 8. LIMITATIONS

While RSUD20K aims to facilitate the development of road scene understanding algorithms tailored for autonomous driving, it does have certain limitations that warrant consideration. The dataset does not extensively address the fine-grained recognition of objects commonly encountered in everyday driving scenarios. For instance, a micro bus might serve as a police vehicle or even operate as an ambulance. Similarly, trucks come in various shapes and sizes, each serving a distinct purpose. While our work establishes a foundational set of objects for autonomous driving, a potential next step is to identify and collect images for these diverse use-cases.

## 9. ADDITIONAL RESULTS

In Figs. 8 and 9, we present additional experimental results on RSUD20K, showcasing model predictions and examples of driving scenes on Bangladesh roads.

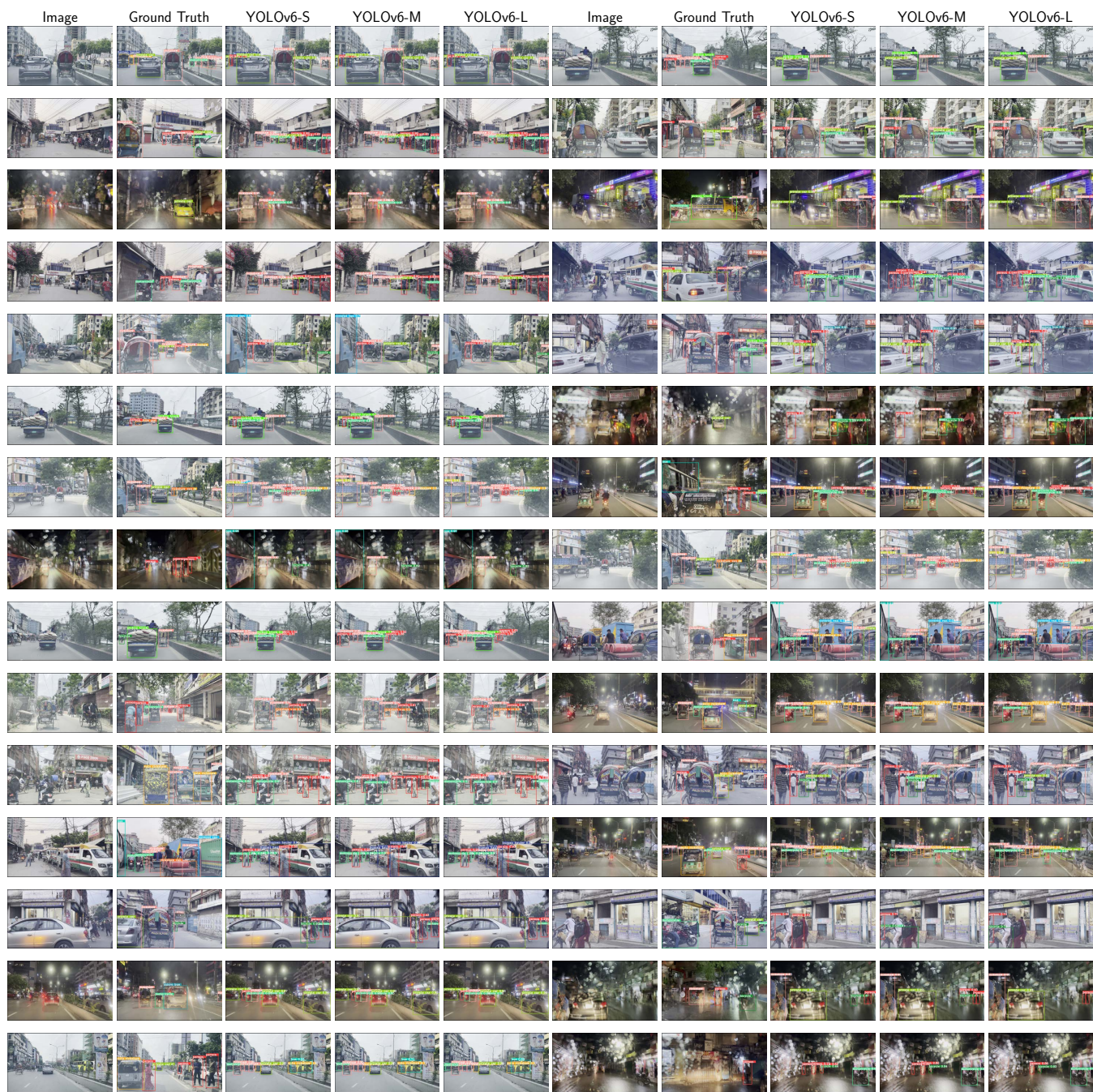


**Fig. 8: Visualization comparison of predictions by state-of-the-art object detectors on RSUD20K. Zoom-in for better details.**



**Fig. 9: Randomly selected instances from RSUD20K dataset for road scene understanding in Bangladesh.** The dataset consists of a total of **20334** images with **130K** bounding box annotations of **13** different objects. Images are captured from the driving perspective of diverse road scenes, objects from different viewpoints, occlusions, as well as under various weather conditions.